microRNA-29a inhibits cardiac fibrosis in Sprague-Dawley rats by downregulating the expression of DNMT3A

Run-He Qin, Hui Tao, Shi-Hao Ni, Peng Shi, Chen Dai, Kai-Hu Shi[1]

Department of Cardiothoracic Surgery, The Second Hospital of Anhui Medical University; Anhui-*China*
[1]Department of Cardiothoracic Surgery, Affiliated Hospital of Integrated Traditional Chinese and Western Medicine, Nanjing University of Chinese Medicine; Nanjing-*China*

Abstract

Objective: This study aims to investigate the effect of miR-29a targeting the regulation of DNMT3A on the development of cardiac fibrosis in Sprague-Dawley (SD) rats.
Methods: *In vivo* experiment: SD rats were randomly divided into model and control groups. The cardiac and left ventricular indices in each group were calculated. The pathological changes of the myocardium were observed. The expression levels of miR-29a, ColIA1, α-SMA, and DNMT3A in the myocardium of each group were detected. *In vitro* experiment: The cardiac fibroblasts (CFs) of SD rats were isolated from the myocardial tissue of SD rats and cultured. The miR-29a mimics, inhibitors, DNMT3A-siRNA, and control-siRNA were transfected into CFs. The expression levels of miR-29a, DNMT3A, ColIA1, and α-SMA were detected, and the proliferation of CFs after transfection was observed.
Results: The heart weight index of the rats in the model group increased significantly compared with that in the control group. Obvious collagen deposition was observed in the myocardial tissue of the model group. The expression levels of ColIA1, α-SMA, and DNMT3A in the model group were significantly higher than those in the control group ($p<0.05$).
Conclusion: miR-29a reduced the activation and proliferation of CFs to improve cardiac fibrosis probably by the downregulation of DNMT3A. *(Anatol J Cardiol 2018; 20: 198-205)*
Keywords: miR-29a, DNMT3A, cardiac fibroblasts, cardiac fibrosis

Introduction

Cardiac fibrosis is the pathological process of abnormal collagen fibrous deposition in the interstitial cells of cardiac fibroblasts (CFs) caused by various damage factors. Cardiac fibrosis is an important risk factor and pathological basis for the development of heart failure and other heart diseases (1). CFs are the main source of extracellular matrix in cardiac fibrosis. Therefore, inhibition of the activation and proliferation of CFs is the key to inhibit cardiac fibrosis (2, 3). The activation of CFs is mainly manifested by the enhancement of cell proliferation and upregulation of type I collagen and a-SMA. Our previous studies have shown that DNA methyltransferase enzymes A (DNMT3A) can upregulate the signal transduction pathway and promote cardiac cell fibrosis by silencing the expression of Ras-association domain family 1 isoform A (RASSF1A) (4-6). DNMT participates in the regulation of gene transcription and in gene inactivation, disease development, and other processes (7-9).

MicroRNAs (miRNAs or miRs) are a class of small fragments of non-coded RNA that regulate the expression of target genes at the transcriptional level. Previous studies have shown that miR-29a can participate in pathophysiological processes, such as cell proliferation, apoptosis, canceration, and fibrosis, by regulating the target gene (10-14). Reportedly, DNMT3A is one of the target genes of miR-29a, and miR-29a is essential in maintaining hematopoietic stem cells function and mediates its effects by modulating the activity of the epigenetic regulator DNMT3A (15). However, it remains unclear whether miR-29a can affect cardiac fibrosis by regulating the expression of DNMT3A.

In the present study, we observed the expression changes of miR-29a and its potential target gene DNMT3A in CFs during cardiac fibrosis and explored the effect of their regulatory relationships on the process of cardiac fibrosis in SD rats.

Address for correspondence: Kai-Hu Shi, MD, Department of Cardiothoracic Surgery, The Second Hospital of Anhui Medical University; Anhui 23060 Hefei-*China*
Phone: 86-551-63869420 E-mail: m18855193667@163.com
Accepted Date: 24.05.2018 **Available Online Date:** 11.09.2018

DOI:10.14744/AnatolJCardiol.2018.98511

Methods

Animal experiment

Sixty healthy adult male Sprague-Dawley (SD) rats (8 weeks old, 150-170 g) and healthy infant SD rats (5–7 days old, 20–22 g) were purchased from Animal Laboratory Center. The rats were placed in a comfortable and quiet room for 1 week before the initiation of the experimental procedure. The adult male SD rats were randomly divided into normal and cardiac fibrosis model groups; there were 30 rats in each group. The inducer 0.5% isoproterenol (ISO, 5 mg/kg.d) was subcutaneously injected into the rats in the model group once a day for 7 days to establish a cardiac fibrosis model. An equal dose of saline was administered to the control group once a day for 7 days. The rats were weighed after 12 h of fasting and water prohibition on the sixth experiment day. The rats were sacrificed after administering anesthesia, and cardiac specimens of the middle section of the middle left ventricle at 5 mm from the apex were taken and embedded with paraffin. The specimens were cut into continuous slice (5 μm), and rat serum was collected. Cardiac and left ventricular indices of each group were calculated. The pathological changes of the myocardium were observed by Hematoxylin-eosin (H&E) and Masson staining.

Extraction and culture of CFs from infant SD rats

Infant SD rats were soaked in alcohol for sterilization, they were executed and the heart was removed under aseptic operation and rinsed two times with a pre-cooled phosphate buffer. The hearts were transferred to a 5-mL EP tube carefully and cut with the scissors; they were digested with a mixed enzyme solution (trypsin:collagenase I ratio, 2:1). The extracted cells were cultured in DMEM medium containing 10% fetal bovine serum, and adherent cells were identified as CFs using an inverted microscope and immunohistochemical methods. The medium was replaced for continuous cultivation and passage at 37°C with 5% CO_2.

This study was audited and approved by the Animal Ethics Committee. All experimental procedures and animal care were performed under the guidance of the Ethics Committee in order to minimize the suffering of animals.

Transfection and drug treatment

The miR-29a mimics and control-siRNA were transfected into CFs. The cells were digested and made into a cell suspension (5×10^4/mL). They were added into 6-well plates (2 mL/well) and cultured at 37°C with 5% CO_2. They were used for transfection when cell fusion reached up to 30%–50%. The miR-29a mimics and control-siRNA were mixed with Lipofectamine™ 2000 according to the kit protocol, which were transfected into CFs and cultured at 37°C with 5% CO_2 for 24 h. At the same time, they were treated with DNMT3A inhibitor and PDGF-BB, respectively, in other 6-well plates, and the medium were changed to a medium with 2 μM 5-AzadC or 10 ng/mL PDGF-BB after culture overnight, the cells were cultured for 48 h continuously.

RNA extraction and reverse transcription-quantitative polymerase chain reaction (RT-qPCR)

The cells were harvested after transfection for 48 h, and they were washed with RNase-free PBS. Total RNA was extracted using an RNeasy Mini kit (cat. no. 74104; Qiagen China Co., Ltd., Shanghai, China) according to the manufacturer's protocol. RNA concentration and purity were detected using a Qubit Fluorometer (Thermo Fisher Scientific, Inc, Shanghai, China). A total of 1 μg RNA was subjected to reverse transcription using a GenePharma Hairpin-it™ miRNAs RT-PCR Quantitation Kit. qPCR was performed using ABI Step One Real-time PCR (ABI Inc., Illinois, USA), and the primers used are presented in Table 1. The quantification method used was the 2-ΔΔCq method as described previously. The β-actin gene was used as an internal control. The thermocycling conditions were as follows: pre-degeneration at 95°C for 10 min, followed by 40 cycles of degeneration at 95°C for 12 s, annealing at 60°C for 20 s, and extension at 72°C for 30 s.

Immunohistochemical test

The 5-μm cardiac tissue slices were incubated with 0.3% endogenous peroxidase blocking solution for 20 min after dewaxing and hydration, then they were incubated with 3% hydrogen peroxide solution at room temperature for 10 min. The slices were washed with PBS three times (3 min/time). Antigen retrieval was performed using citrate buffer (pH 6.0) at 121°C for 2 min. The cells were incubated with primary monoclonal antibodies (1:100 anti-ColIA1, 1:200 anti-DNMT3A, and 1:100 anti-a-SMA) at 4°C overnight after blocking with 5% BSA for 2 h at room temperature. The cells were then sequentially incubated with rabbit anti-mouse and goat anti-rabbit non-biotinylated regents (Zhongshanjinqiao, Beijing, China) according to the manufacturer's instructions, and they were observed under a microscope and analyzed with a photo and image auto analysis system (Image-Pro Plus, China).

Western blotting test

Total protein was extracted from the cells after they were transfected for 48 h. The transfected cells were lysed with radioimmunoprecipitation assay lysis buffer (PBS containing 1% NP40, 0.1% SDS, 5 mM EDTA, 0.5% sodium deoxycholate, 1 mM

Table 1. Primers used in this study

Genes	Sequences (5′-3′)
α-SMA	F: TGGCCACTGCTGCTTCCTCTTCTT
	R: GGGGCCAGCTTCGTCATACTCCT
Col1A1	F: GGAGAGAGCATGACCGATGG
	R: GGGACTTCTTGAGGTTGCCA
DNMT3a	F: GCTCTAGACGAAAAGGGTTGGACATCAT
	R: GCTCTAGAGCCGAGGGAGTCTCCTTTTA
β-actin	F: TGGAATCCTGTGGCATCCATGAAAC
	R: ACGCAGCTCAGTAACAGTCCG

Anatol J Cardiol 2018; 20: 198-205
DOI:10.14744/AnatolJCardiol.2018.98511

sodium orthovanadate, and protease inhibitors) on ice for 30 min with shaking at 12,000 rpm/min. Total proteins were isolated, and the concentration was determined using a BCA Kit. Proteins (40 μg/lane) were separated using 10% SDS-PAGE electrophoresis. Then, the gel was electrotransferred to a PVDF membrane. The PVDF membrane was rinsed with TBS for 10–15 min, placed in TBS/T blocking buffer containing 5% (w/v) skimmed milk powder, and shaken at room temperature for 1 h. The membrane was incubated at 4°C overnight after adding primary antibodies. Then, the membrane was washed with TBST three times (5 min each time). The membrane was incubated at 37°C for 1 h with IgG-HRP secondary antibody (1:10000). The membrane was developed with ECL (Perkin-Elmer Inc.) for 5 min. The protein bands were quantified as a ratio to β-actin using Imagequant LAS4000 (GE Healthcare China).

Detection of CF proliferation by MTT colorimetric method

The cells after transfection for 48 h were seeded onto four 96-well plates. Each group of cells was provided with five repeated wells, each of which was inoculated with 1×10^4 cells/well. The plates were cultivated at 37°C with 5% CO_2 for 2 days after inoculation, one plate was taken out. In total, 50 μL of 1×MTT (5 mg/mL) was added in each sample well at 12, 24, and 48 h, and the cells were incubated for an additional 4 h at 37°C. Of note, 150 μL DMSO was added in each sample well after the culture medium was discarded. The optical density of each sample hole was measured using a microplate reader at 490 nm after shaking for 10 min. The negative control group only contained medium. The experiment was repeated three times.

ELISA test

The concentrations of PICP, PIIINP, and PDGF-BB in serum were detected using PICP ELISA (R&D Systems, USA), PIIINP ELISA (Uscn Life Science Inc., Wuhan, China), and PDGF-BB ELISA kits (R&D Systems, USA), respectively. The measurements were performed according to the kit manual. OD450 values were detected using a microplate reader (Thermo Fisher, USA).

Luciferase activity assay

The 3′-UTR region of the DNMT3a gene was amplified by PCR and inserted into a pGL3 vector (Promega Corporation, Madison, WI, USA). A pGL3 construct containing DNMT3a 3′-UTR with point mutations in the seed sequence was synthesized using 30 reactions of the Quik-Change Lightning Site-Directed Mutagenesis kit (Agilent Technologies, Inc., Santa Clara, CA, USA) according to the manufacturer's protocol. HEK293 cells and rats CFs were cultured in 24-well plates, and the cells (2×10^5) were transfected with the recombinant plasmid pGL3 via Lipofectamine™ 2000. The cells were collected after transfection for 48 h and split with reporter gene cell lysis buffer (Beyotime Institute of Biotechnology). The luciferase activity levels were detected using a dual luciferase reporter assay system (Promega Corporation). Relative luciferase activity levels were normalized to Renilla luciferase activity levels, which served as an internal control.

Statistical analysis

All analyses were performed using SPSS 20.0 software (SPSS Inc., Chicago, USA). Normality testing of data was performed using the Shapiro–Wilk test. The quantitative data of normal distribution were expressed as $\bar{x}\pm s$. The differences among the groups were analyzed by one-way analysis of variance or Student's t-test. Pairwise comparison of multiple groups was performed using Dunnett's t-test. The quantitative data of skewed distribution among groups were compared using a nonparametric test. When the difference between groups was statistically significant, pairwise comparisons, which were performed by the nonparametric test, were performed in multiple groups. P values <0.05 were considered statistically significant.

Results

Biochemical indices and pathological changes of myocardium in rats

H&E and Mason staining results showed that myocardial collagen deposition occurs in myocardial tissues (Fig. 1a).

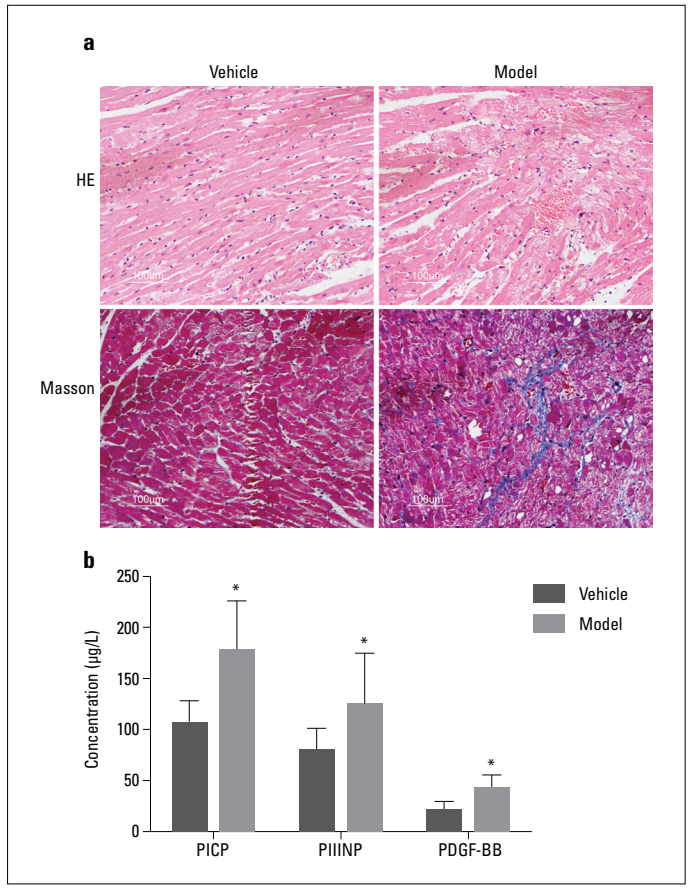

Figure 1. Pathological changes of myocardial tissue and serum biochemical indices in rats after ISO treatment
(a) H&E and Mason staining results show that myocardial collagen deposition appears in myocardial tissues. (b) ELISA results show that PDGF-BB, PICP, and PIIINP concentrations are significantly higher in ISO-treated rats than in normal control rats (*P<0.001 vs. control, n=30)

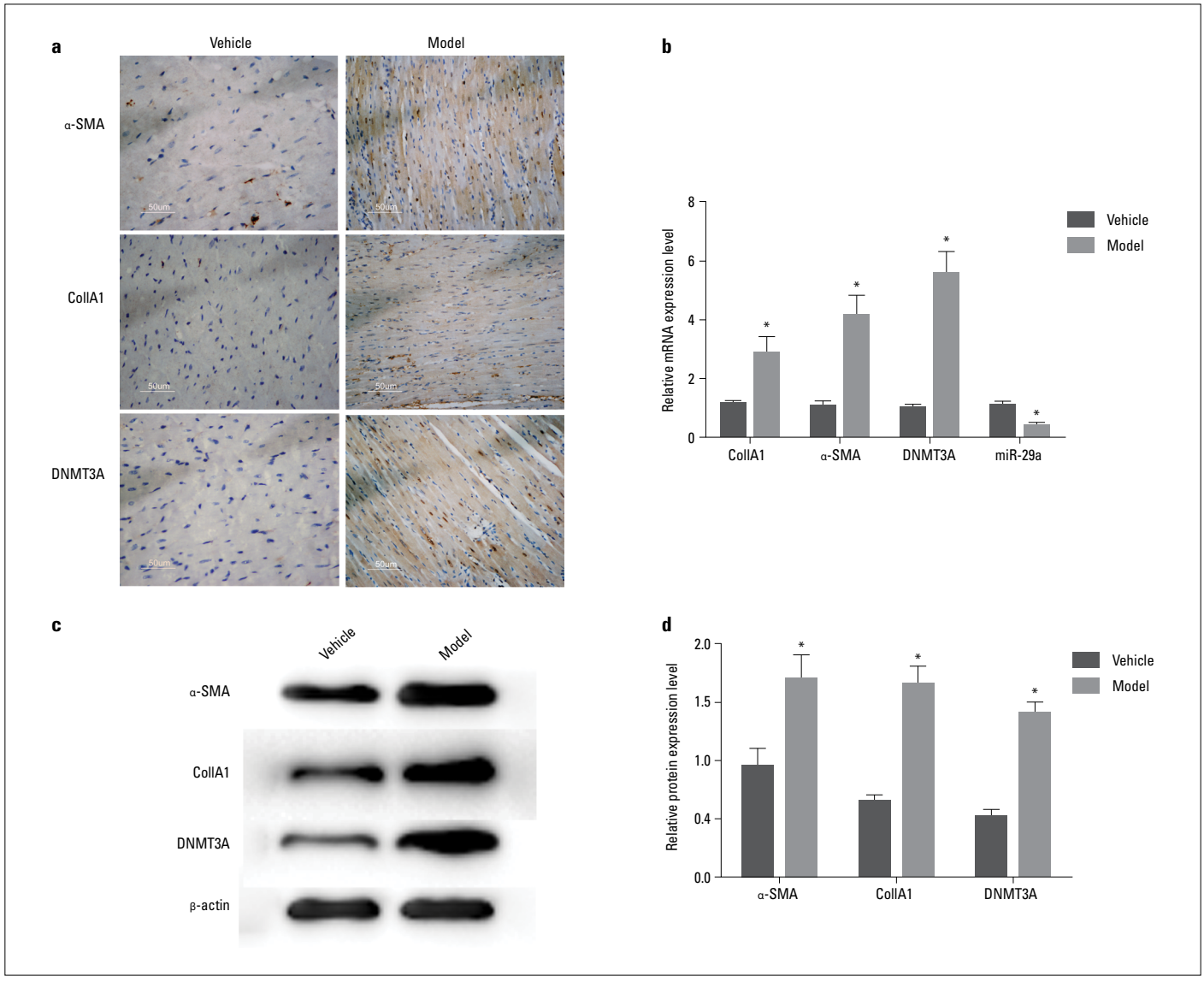

Figure 2. The expression changes of CollA1, α-SMA, DNMT3A, and miR-29a in myocardial tissue of rats after ISO treatment
(a) The immunohistochemical results show that the protein expression levels of CollA1, α-SMA, and DNMT3A in the model group are higher than those in the control group. (b) RT-PCR results show that the mRNA expression levels of CollA1, α-SMA, and DNMT3A increase, whereas the mRNA expression level of miR-29a decreases in the model group. (c, d) Western blotting results also show that the protein expression levels of CollA1, α-SMA, and DNMT3A in the model group are higher than those in the control group (*P<0.001 vs. control, n=30)

Table 2. Comparison of the PICP, PIIINP, and PDGF-BB content between vehicle and model groups

	Vehicle (n=30)	Model (n=30)	*P* value
PICP (μg/L)	45.36±12.5	21.57±7.14	<0.001
PIIINP (μg/L)	194.52±48.63	112.74±31.56	<0.001
PDGF-BB (μg/L)	128.63±38.64	81.55±24.68	<0.001

ELISA results showed that PDGF-BB (45.36±12.5 vs. 21.57±7.14, p<0.001), PICP (194.52±48.63 vs. 112.74±31.56, p<0.001), and PIIINP (128.63±38.64 vs. 81.55±24.68, p<0.001) concentrations were significantly higher in ISO-treated rats than in normal control rats, which suggests that myocarditis and injury exists in rats in the model group (Fig. 1b, Table 2).

The expression of DNMT3A is upregulated and the expression of miR-29a is downregulated in myocardial tissues with activated CFs.

Immunohistochemistry results showed that the protein expression levels of CollA1, α-SMA, and DNMT3A in the model group were higher than those in the control group (Fig. 2a). RT-PCR results showed that the mRNA expression levels of CollA1, α-SMA, and DNMT3A increased, whereas the mRNA expression level of miR-29a decreased in the model group (Fig. 2b, Table 3). Western blotting results also showed that the protein expression levels of CollA1, α-SMA, and DNMT3A in the model group were higher than those in the control group (Fig. 2c and 2d, Table 4).

Anatol J Cardiol 2018; 20: 198-205
DOI:10.14744/AnatolJCardiol.2018.98511

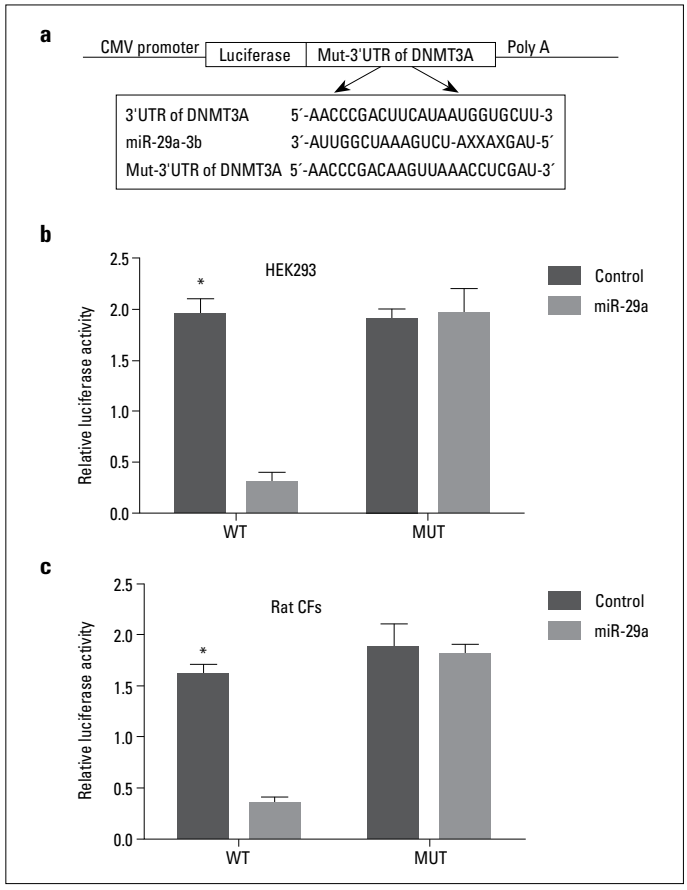

Figure 3. Effects of miR-29a on luciferase activity
(a) The predicted binding site of miR-29a with the DNMT3a 3′-UTR by bioinformatics. (b) In HEK293 cells, miR-29a can inhibit the expression of luciferase activity in the 3′-UTR of wild-type (WT) DNMT3A but cannot inhibit it in the 3′-UTR of mutant (MUT) DNMT3A. (c) In rat CFs, miR-29a can inhibit the expression of luciferase activity in the 3′-UTR of WT DNMT3A but cannot inhibit it in the 3′-UTR of MUT DNMT3A (*P<0.001 vs. control, n=6)

Table 3. Comparison of the mRNA expression levels of ColIA1, α-SMA, and DNMT3A between vehicle and model groups

	Vehicle (n=30)	Model (n=30)	*P* value
ColIA1	1.13±0.14	2.35±0.24	<0.001
α-SMA	1.21±0.32	4.17±1.56	<0.001
DNMT3A	1.14±0.22	4.85±1.68	<0.001
miR-200a	1.13±0.18	0.31±0.14	<0.001

TargetScan was used to identify the potential targets of miR-29a. An important enzyme in DNA methylation, DNMT3a, was identified as one of the potential targets of miR-29a. The predicted binding site of miR-29a with the DNMT3a 3′-UTR is shown in Figure 3a. To examine miR-29a–DNMT3a interactions, DNMT3a complementary sites, with or without mutations, were cloned into the 3′-UTR of the firefly luciferase gene and co-transfected with miR-29a mimics or a negative control in HEK293 cells and rat CFs. The presence of miR-29a led to a significant reduction in the relative luciferase activity levels in the wild-type construct of the DNMT3a 3′-UTR in HEK293 cells (Fig. 3b) and rat CFs (Fig. 3c).

Table 4. Comparison of the protein levels of ColIA1, α-SMA, and DNMT3A between vehicle and model groups

	Vehicle (n=30)	Model (n=30)	*P* value
ColIA1	0.93±0.19	1.63±0.32	<0.001
α-SMA	0.62±0.05	1.57±0.26	<0.001
DNMT3A	0.55±0.08	1.48±0.18	<0.001

miR-29a can inhibit the proliferation of activated rat CFs and downregulate the expression of fibrosis-related indices

After PDGF-BB treatment, the proliferation of rat CFs was enhanced and the expression levels of DNMT3A, ColIA1, and α-SMA increased. The transfection of miR-29a can inhibit the proliferation of CFs and the expression of DNMT3A, ColIA1 and α-SMA, the effects of which were the same as that of DNMT3A inhibitors (Fig. 4; Tables 5, 6, and 7).

Discussion

It is thought that cardiac fibrosis is associated with arrhythmia (particularly atrial fibrillation), cardiac insufficiency, and myocardial hypertrophy, among others (16). Exploring the pathogenesis of these diseases and determining effective treatment are important to prevent and suppress the development of cardiac fibrosis. The activation and proliferation of CFs and the related phenotypic transformations are important in the formation of cardiac fibrosis (2). CFs activate and proliferate due to various pathogenic factors, and the synthesis and secretion of extracellular matrix are increased, which lead to the deposition of extracellular matrix, such as α-SMA and collagen I, further promoting fibrosis (17).

Previous studies have found that DNA methylation is involved in the development of cardiac fibrosis. DNMT3A is a DNA methylation catalytic enzyme, and it plays an important role in the fibrosis process (18). The upregulated expression of DNMT3A leads to excessive methylation of the genome of CFs, and TGF-β can promote the methylation of related DNA fragments in cardiac fibrosis and the differentiation of fibrous cells into fibroblasts as well as collagen deposition (19, 20). In addition, it was found that miR-29a is involved in the negative regulation of cardiac fibrosis (21-23). In the present study, we found that the expression level of miR-29a decreased and the expression levels of DNMT3A, ColIA1, and α-SMA increased in an SD rat model of cardiac fibrosis. At the cellular level, we found that miR-29a can directly act on the 3′-UTR of DNMT3A to inhibit the expression of DNMT3A. The transfection of miR-29a into rat CFs activated by PDGF-BB can inhibit their proliferation ability and the expression of DNMT3A, ColIA1 and α-SMA in the cells. This suggests that miR-29a directly acts on the 3′-UTR of DNMT3A

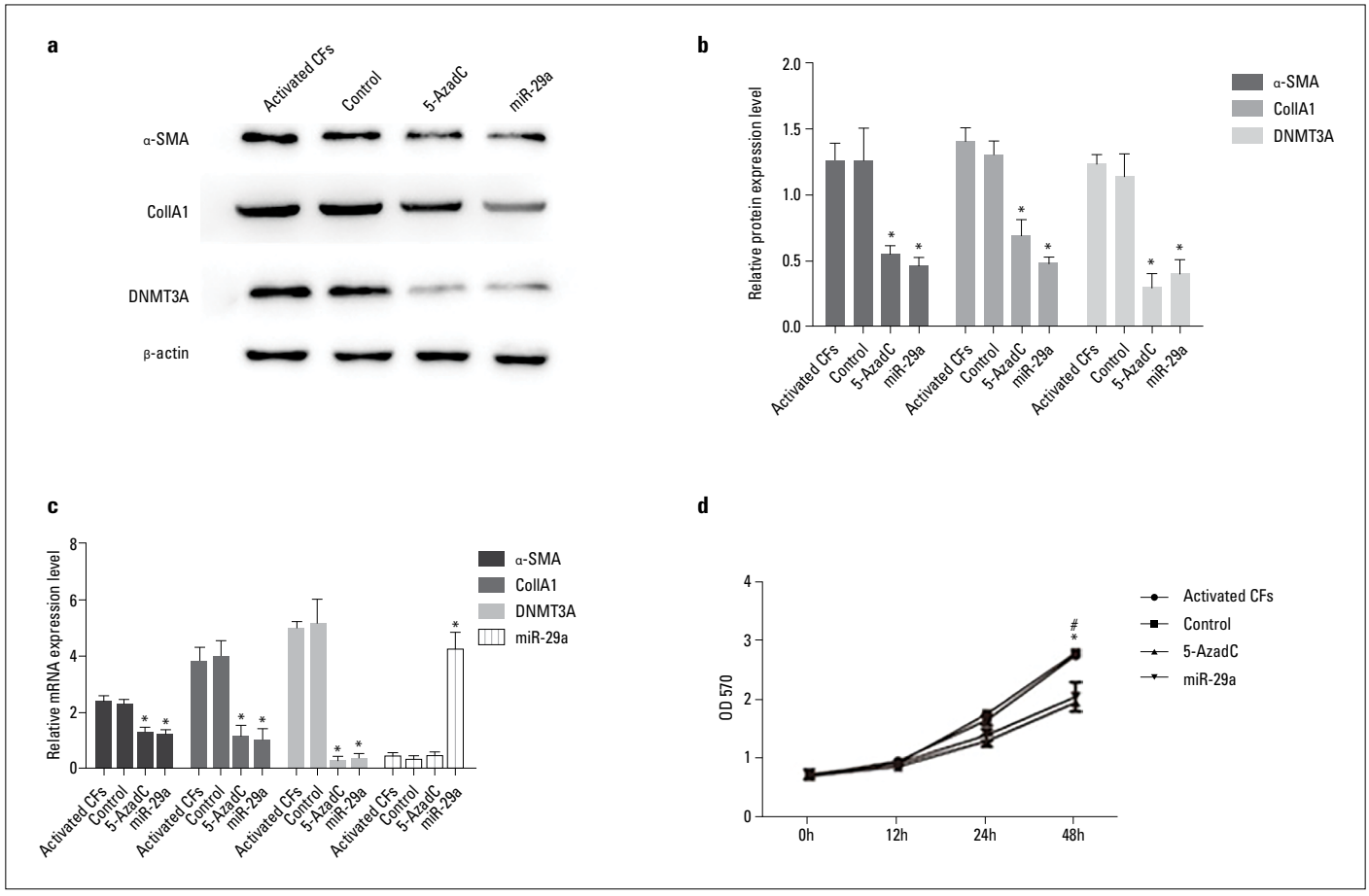

Figure 4. miR-29a can inhibit the proliferation of activated rat cardiac fibroblasts and the expression of fibrosis-related indices
(a, b) Western blotting results show that miR-29a can inhibit the protein expression of DNMT3A, ColIA1, and α-SMA in activated cardiac fibroblasts in rats (*P<0.001 vs. control, n=6). (c) RT-PCR results show that miR-29a can inhibit the mRNA expression of DNMT3A, ColIA1, and α-SMA in activated cardiac fibroblasts in rats (*P<0.001 vs. control, n=6). (d) miR-29a can inhibit cell proliferation *#P<0.05 vs. control, n=6

Table 5. Comparison of the protein levels of ColIA1, α-SMA, and DNMT3A among different groups (n=6)

	Activated CFs	Control	5-Azadc	miR-29a
ColIA1	1.35±0.23	1.37±0.31[1]	0.51±0.08*	0.49±0.07*
α-SMA	1.49±0.17	1.38±0.17[2]	0.63±0.09*	0.51±0.05*
DNMT3A	1.33±0.10	1.29±0.14[3]	0.29±0.09*	0.38±0.08*

([1]P=0.938 vs. control, [2]P=0.472 vs. control, [3]P=0.708 vs. control, *P<0.001 vs. control, n=6)

Table 6. Comparison of the mRNA expression levels of ColIA1, α-SMA, DNMT3A, and miR-29a among different groups (n=6)

	Activated CFs	Control	5-Azadc	miR-29a
ColIA1	2.31±0.23	2.24±0.09[1]	1.15±0.07*	1.12±0.08*
α-SMA	3.74±0.63	3.97±0.95[2]	0.88±0.21*	0.84±0.16*
DNMT3A	4.42±0.14	4.41±1.18[3]	0.24±0.08*	0.29±0.08*
miR-29a	0.41±0.04	0.39±0.06[4]	0.42±0.06	3.87±0.74*

([1]P=0.649 vs. control, [2]P=0.744 vs. control, [3]P=0.973 vs. control, [4]P=0.720 vs. control, *P<0.001 vs. control, n=6)

Anatol J Cardiol 2018; 20: 198-205
DOI:10.14744/AnatolJCardiol.2018.98511

Table 7. MTT analysis of the proliferation of CFs in different groups (n=6)

	Activated CFs	Control	5-Azadc	miR-29a
0 h	0.667±0.072	0.652±0.061	0.671±0.075	0.664±0.055
12 h	0.776±0.091	0.771±0.094	0.742±0.079	0.715±0.063
24 h	1.374±0.142	1.301±0.115	0.972±0.117	1.054±0.117
48 h	2.342±0.056	2.438±0.067	1.561±0.089	1.644±0.241*#

(P=0.347, activated CFs vs. control; *P<0.001, miR-29a vs. control, n=6; #P<0.001, miR-29a vs. activated CFs)

to inhibit cardiac fibrosis. In another study, it was found that the overexpression of miR-29a attenuates the ANG-induced upregulation of Sp1 levels and collagen in cardiac myofibroblasts, and miR-29a could abrogate cardiac fibrosis through the suppression of profibrogenic transcription factor Sp1 (24). In contrast, other studies have suggested that the inhibition of miR-29a is effective in improving ventricular remodeling and hypertrophy caused by pressure overload, and the miR-29a antagomir reduces pressure over load-induced cardiac fibrosis in mice (25, 26).

miRNAs are a class of small, single-stranded RNAs with 18-24 nucleotides; they are widely found in eukaryotes, with high conservatism, scheduling, and tissue specificity. They can regulate gene expression by inhibiting transcription or cutting the target gene RNA. A previous study showed that the expression level of miR-29a decreases in many types of tumors, the upregulation of miR-29a can inhibit the proliferation of tumor cells, and it has the role of a tumor suppressor gene (24). miR-29a has also been associated with fibrosis of various organs (21-23). In the present study, we confirmed that miR-29a is also associated with cardiac fibrosis and may be a target for controlling cardiac fibrosis.

Genomic stability is mainly regulated by genetic and epigenetic mechanisms. Promoter methylation mediated by DNMT is the main cause of gene inactivation. In the present study, we found that the expression level of DNMT in the myocardium of rats with fibrosis increases, whereas the expression of miR-29a, which can inhibit DNMT expression, significantly decreases. Our previous study had shown that DNMT3A can increase the expression of RASSF1A and activate the Ras/ERK1/2 signaling pathway (4). In the present study, the expression level of RASSF1A and ERK1/2 in activated CFs after the transfection of miR-29a was significantly decreased. This suggests that miR-29a inhibits the Ras/ERK1/2 signaling pathway in CFs by silencing DNMT3A, thus inhibiting the activation and proliferation of CFs.

Conclusion

In conclusion, we found that miR-29a can control the activation of myocardial cells and decrease the level of cardiac fibrosis by the downregulation of DNMT3A expression and inhibition of the Ras/ERK1/2 signaling pathway. DNMT3A may be an epigenetic treatment target for cardiac fibrosis.

Acknowledgements: This work was supported by the National Natural Science Fund (81570295).

Conflict of interest: None declared.

Peer-review: Externally peer-reviewed.

Authorship contributions: Concept – K.S.; Design – K.S., R.Q.; Supervision – K.S.; Fundings – P.S., C.D.; Materials – P.S.; Data collection &/or processing – H.T., S.N.; Analysis &/or interpretation – K.S., R.Q.; Literature search – K.S., R.Q.; Writing – R.Q., C.D.; Critical review – K.S.

References

1. Nagpal V, Rai R, Place AT, Murphy SB, Verma SK, Ghosh AK, Vaughan DE: MiR-125b Is Critical for Fibroblast-to-Myofibroblast Transition and Cardiac Fibrosis. Circulation 2016; 133: 291-301.
2. Gupta SS, Zeglinski MR, Rattan SG, Landry NM, Ghavami S, Wigle JT, et al. Inhibition of autophagy inhibits the conversion of cardiacfibroblasts to cardiac myofibroblasts. Oncotarget 2016; 7: 78516-31.
3. Ng KM, Mok PY, Butler AW, Ho JC, Choi SW, Lee YK, et al. Amelioration of X-Linked Related Autophagy Failure in Danon Disease With DNA Methylation Inhibitor. Circulation 2016; 134:1373-89. [CrossRef]
4. Tao H, Yang JJ, Chen ZW, Xu SS, Zhou X, Zhan HY, et al. DNMT3A silencing RASSF1A promotes cardiac fibrosis through upregulation of ERK1/2. Toxicology 2014; 323: 42-50. [CrossRef]
5. Pan X, Chen Z, Huang R, Yao Y, Ma G. Transforming Growth Factor β1, Induces the Expression of Collagen Type I by DNA Methylation in Cardiac Fibroblasts. PLoS One 2013; 8: e60335. [CrossRef]
6. Jjingo D, Conley AB, Yi SV, Lunyak VV, Jordan IK. On the presence and role of human gene-body DNA methylation. Oncotarget 2012; 3: 462-74. [CrossRef]
7. He M, Fan J, Jiang R, Tang WX, Wang ZW. Expression of DNMTs and genomic DNA methylation in gastric signet ring cell carcinoma. Mol Med Rep 2013; 8: 942-8. [CrossRef]
8. Mirza S, Sharma G, Parshad R, Gupta SD, Pandya P, Ralhan R. Expression of DNA methyltransferases inbreast cancer patients and to analyze the effect of natural compounds on DNA methyltransferases and associated proteins. J Breast Cancer 2013; 16: 23-31.
9. Mateescu B, Batista L, Cardon M, Gruosso T, de Feraudy Y, Mariani O, et al. miR-141 and miR-29a act on ovarian tumorigenesis by controlling oxidative stress response. Nat Med 2011; 17: 1627-35.
10. Zhang Z, Shen S. Combined low miRNA-29s is an independent risk factor in predicting prognosis of patients with hepatocellular carcinoma after hepatectomy: A Chinese population-based study. Medicine (Baltimore) 2017; 96: e8795. [CrossRef]

11. Liu S, Zhang X, Hu C, Wang Y, Xu C. miR-29a inhibits human retinoblastoma progression by targeting STAT3. Oncol Rep 2018; 39: 739-46.
12. Catanzaro G, Sabato C, Russo M, Rosa A, Abballe L, Besharat ZM, et al. Loss of miR-107, miR-181c and miR-29a-3p Promote Activation of Notch2 Signaling in Pediatric High-Grade Gliomas (pHGGs). Int J Mol Sci 2017; 18. pii: E2742. [CrossRef]
13. Ning JZ, Li W, Cheng F, Yu WM, Rao T, Ruan Y, et al. MiR-29a Suppresses Spermatogenic Cell Apoptosis in Testicular Ischemia-Reperfusion Injury by Targeting TRPV4 Channels. Front Physiol 2017; 8: 966. [CrossRef]
14. Tan C, Yu C, Song Z, Zou H, Xu X, Liu J. Expression of MicroRNA-29a Regulated by Yes-Associated Protein Modulates the Neurite Outgrowth in N2a Cells. Biomed Res Int 2017; 2017: 5251236. [CrossRef]
15. Hu W, Dooley J, Chung SS, Chandramohan D, Cimmino L, Mukherjee S, et al. miR-29a maintains mouse hematopoietic stem cell self-renewal by regulating Dnmt3a. Blood 2015; 125: 2206-16. [CrossRef]
16. Dzeshka MS, Lip GY, Snezhitskiy V, Shantsila E. Cardiac fibrosis in patients with atrial fibrillation: mechanisms and clinical implications. J Am Coll Cardiol 2015; 66: 943-59. [CrossRef]
17. Tao H, Yang JJ, Shi KH, Deng ZY, Li J. DNA methylation in cardiac fibrosis: new advances and perspectives. Toxicology 2014; 323: 125-9. [CrossRef]
18. Watson CJ, Collier P, Tea I, Neary R, Watson JA, Robinson C, et al. Hypoxia-induced epigenetic modifications are associated with cardiac tissue fibrosis and the development of a myofibroblast-like phenotype. Hum Mol Genet 2014; 23: 2176-88. [CrossRef]
19. Baas R, van Teeffelen HAAM, Tjalsma SJD, Timmers HTM. The mixed lineage leukemia 4 (MLL4) methyltransferase complex is involved in transforming growth factor beta (TGF-β)-activated gene transcription. Transcription 2018; 9: 67-74. [CrossRef]
20. Elkouris M, Kontaki H, Stavropoulos A, Antonoglou A, Nikolaou KC, Samiotaki M, et al. SET9-Mediated Regulation of TGF-β Signaling Links Protein Methylation to Pulmonary Fibrosis. Cell Rep 2016; 15: 2733-44. [CrossRef]
21. Roncarati R, Viviani Anselmi C, Losi MA, Papa L, Cavarretta E, Da Costa Martins P, et al. Circulating miR-29a, among other up-regulated microRNAs, is the only biomarker for both hypertrophy and fibrosis in patients with hypertrophic cardiomyopathy. J Am Coll Cardiol 2014; 63: 920-7. [CrossRef]
22. Zanotti S, Gibertini S, Curcio M, Savadori P, Pasanisi B, Morandi L, et al. Opposing roles of miR-21 and miR-29 in the progression of fibrosis in Duchenne muscular dystrophy. Biochim Biophys Acta 2015; 1852: 1451-64. [CrossRef]
23. Ntelios D, Meditskou S, Efthimiadis G, Pitsis A, Nikolakaki E, Girtovitis F, et al. Elevated plasma levels of miR-29a are associated with hemolysis in patients with hypertrophic cardiomyopathy. Clin Chim Acta 2017; 471: 321-6. [CrossRef]
24. Ye H, Ling S, Castillo AC, Thomas B, Long B, Qian J, et al. Nebivolol induces distinct changes in profibrosis microRNA expression compared with atenolol, in salt-sensitive hypertensive rats. Hypertension 2013; 61: 1008-13. [CrossRef]
25. Han W, Han Y, Liu X, Shang X. Effect of miR-29a inhibition on ventricular hypertrophy induced by pressure overload. Cell Biochem Biophys 2015; 71: 821-6. [CrossRef]
26. Wang JY, Zhang Q, Wang DD, Yan W, Sha HH, Zhao JH, et al. MiR-29a: a potential therapeutic target and promising biomarker in tumors. Biosci Rep 2018; 38. pii: BSR20171265. [CrossRef]